29th International Cosmic Ray Conference Pune (2005) 2, 1-4

Effects of different solar wind speed profiles in the heliosheath on the modulation of cosmic ray and anomalous protons

U.W. Langner[a,b], M.S. Potgieter[a], H. Fichtner[b] and T. Borrmann[b]
(a) Unit for Space Physics, North-West University, Potchefstroom 2520, South Africa
(b) Institut für Theoretische Physik IV, Ruhr-Universität Bochum, 44780 Bochum,Germany
Presenter: U. W. Langner (fskuwl@puk.ac.za), ger-langner-U-abs1-sh31-oral

A previously used model for the heliospheric modulation of cosmic rays including a solar wind termination shock (TS) is extended to include an asymmetrically shaped outer modulation boundary, with respect to the Sun. The model includes particle drifts, adiabatic energy changes, diffusion, convection, and a heliosheath. It is used to study the effects on the modulation of protons and anomalous protons for different scenarios of the solar wind speed (V) in the heliosheath, in accordance with the predictions of a three-dimensional time-dependent hydrodynamic model of the heliosphere. This model provides the different scenarios for V in the heliosheath. Significant changes occur for mostly the $A < 0$ polarity cycle at all radial distances in the equatorial plane when the V-profile is changed from an assumed incompressible fluid in the heliosheath, with $V \propto 1/r^2$, to $V \propto 1/r^8$. The TS is predicted markedly more effective in the heliospheric nose region than in the tail region for the $A < 0$ polarity cycle. The different scenarios for V in the heliosheath do not have a substantial effect on the intensities in the $A > 0$ cycle inside the TS. In the heliosheath region, however, the difference can be quite significant, especially at lower energies.

1. Introduction

The interest in the large-scale structure of the heliosphere, in particular the solar wind TS, heliosheath, and heliopause (HP), and the transport of cosmic rays (CRs) within this structure has increased significantly with the *Voyager 1* spacecraft crossing the TS and entering the heliosheath [12]. For reviews on the global structure and geometry of the heliosphere, see Fichtner [3], Zank [13] and Zank and Müller [14]. In order to study the corresponding complex physical system, a TS model, which has been used to demonstrate simultaneously the significance of heliospheric modulation (especially in the heliosheath), for a variety of cosmic ray species [6,7,9] is extended to include asymmetrically shaped heliospheric boundaries. Of particular interest is the shape of the heliopause because it supposedly represents the outer modulation boundary. Langner & Potgieter [8] recognized that assuming the solar wind speed decreases as $V \propto 1/r^2$ beyond the TS, with r the radial distance from the Sun, could be an oversimplification (see also e.g., Florinski et al. [4]). The model is now improved to handle different scenarios of how V may change with radial distance and with latitude in the heliosheath. In order to establish plausible scenarios in the heliosheath for the heliospheric nose and tail regions, a time-dependent three-dimensional hydrodynamic model of the dynamics of the heliosphere is utilized [1]. The combination of the predictions and results of these models is a step closer to a realistic and self-consistent description of heliospheric modulation.

2. Modulation Model

The modulation computations were performed with a model neglecting any azimuthal dependence but which combines all major modulation mechanisms with diffusive shock acceleration at the TS, incorporating a heliosheath within an asymmetrical heliosphere. Haasbroek et al. [5] developed an asymmetrical model which is extended to include a TS by Langner & Potgieter [8]. The model is based on the numerical solution of the time-dependent cosmic ray transport equation [11] and is described in detail by Langner et al. [8, 9, 10]. For the 3D time-dependent hydrodynamic model the standard set of hydrodynamic equations for the

plasma and the neutral gas are used, with the assumption that the magnetic field does not have a direct dynamical influence [1,10]. This work includes a more realistically shaped heliosphere and solar wind profile than used before and gives valuable insights into what happens in the heliosheath, in the nose and tail regions of the heliosphere. For an application to electrons, see Ferreira et al. [2].

3. Modeling results, discussion and conclusions

Figure 1 illustrates the three computed V profiles and the resulting $\nabla.\mathbf{V}$ in the equatorial plane as a function of radial distance r. The $\nabla.\mathbf{V}$ determines the energy losses and gains of CRs in the heliosphere, e.g., $\nabla.\mathbf{V} < 0$ implies acceleration of particles in the heliosheath but not to the same extent as at the TS where its value becomes large negative; $\nabla.\mathbf{V} > 0$ implies adiabatic deceleration of particles, normally occurring inside the TS where it get larger with decreasing radial distances to produce the characteristic E^{1} spectral slopes for nuclei at Earth. For an incompressible fluid $V \propto 1/r^2$, with $\nabla.\mathbf{V} = 0$, so that neither energy losses nor gains for CRs could then play a role in the heliosheath, by far the simplest assumption [6, 7, 9]. The V-profiles in the heliosheath are not arbitrarily chosen but computed with the mentioned hydrodynamic model. The V profiles in the heliosheath used in the asymmetric TS model must therefore be considered well

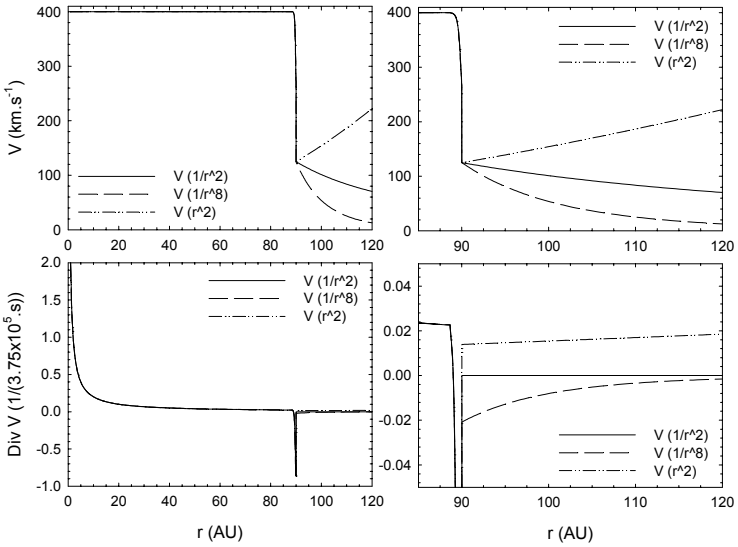

Figure 1. Three computed solar wind speed profiles [1], $V \propto 1/r^2$, and the extreme cases of $V \propto 1/r^8$ and $V \propto r^2$ as a function of radial distance in the equatorial plane from 1 to 120 AU. In the bottom panels the corresponding divergence of V is shown. Right panels show the same as on the left but enlarged for the heliosheath region [10].

informed estimates for given periods. For the first of the three V scenarios, the standard assumption was made that the solar wind is incompressible in this region, resulting in $V \propto 1/r^2$. For the second scenario the hydrodynamic model was again used. An approximation of this calculation, where V changes from $V \propto 1/r^8$ in the heliospheric nose region to $V \propto r^2$ in the heliospheric tail region, as an extreme, was then used as input to the asymmetric TS modulation model.

In Figure 2 the solutions for the differential proton intensity of the asymmetric model are shown for solar minimum conditions ($\alpha = 10°$), during the A < 0 cycle for three possible V scenarios in the heliosheath ($V \propto 1/r^2$, $1/r^8$, and r^2). The results are in the nose direction ($\theta = 90^o$), at the *Voyager 1* trajectory latitude ($\theta = 55^o$), and in the tail direction ($\theta = 270^o$) of the heliosphere. The energy spectra are shown at radial distances of 1 AU, 60 AU, at r_s (90 AU in the nose region, 95 AU at the polar regions, and 100 AU in the tail and re-

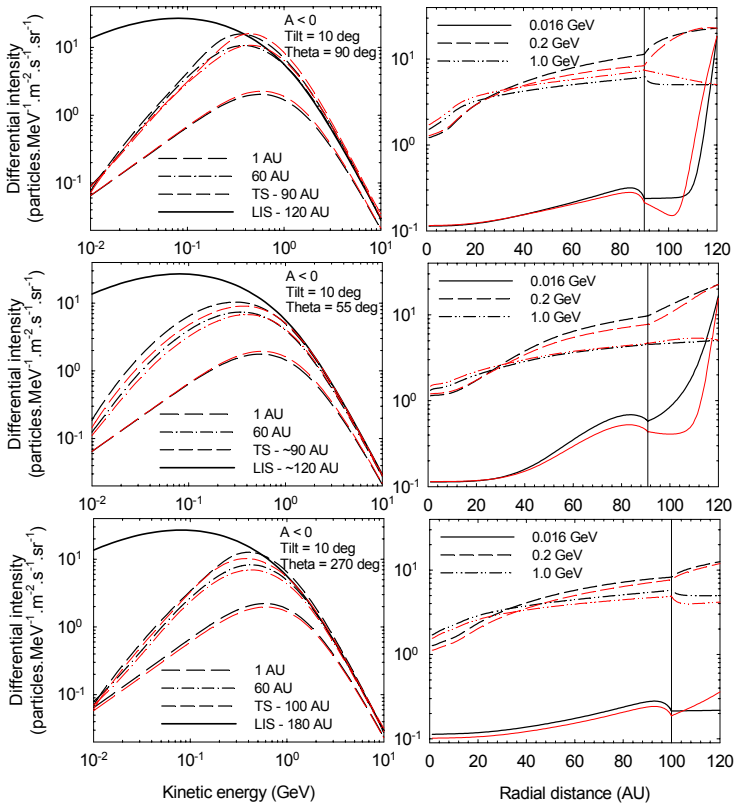

Figure 2. Solutions of the asymmetric model in the nose direction (top panels; $\theta = 90^o$), the *Voyager 1* asymptotic latitude (middle panels; $\theta = 55^o$), and in the tail direction (bottom panels; $\theta = 270^o$); for minimum conditions ($\alpha = 10°$) in the $A < 0$ polarity cycle for different V scenarios in the heliosheath. Left panels: Proton energy spectra at 1 AU, 60 AU, the TS position (90 AU in the nose region, ~90 AU at $\theta = 55^o$, and 100 AU in the tail region) and the HP position (120 AU in the nose, ~120 AU at $\theta = 55^o$, and 180 AU in the tail). Right panels: Differential intensities as function of radial distance at 16 MeV, 200 MeV, and 1 GeV, respectively. The TS position is indicated in the right panels with a vertical line. Black lines are solutions with $V \propto 1/r^2$ in the heliosheath for all latitudes; red lines are solutions with V changing from $V \propto 1/r^8$ in the nose to $V \propto r^2$ in the tail. For colour, see electronic version.

gion) at r_{HP} (120 AU in the nose region, 140 AU at the polar regions, and 180 AU in the tail region) and the differential intensities as a function of radial distance at energies of 16 MeV, 200 MeV, and 1 GeV, respectively For the V-scenarios, first $V \propto 1/r^2$ is assumed in the heliosheath for all latitudes and second that V is changing from $V \propto 1/r^8$ in the heliosheath in the nose direction to $V \propto r^2$ in the heliosheath in the tail direction. In Figure 3 the computations are repeated for anomalous protons.

The different scenarios for V in the heliosheath do not have a substantial effect on the intensities in the $A > 0$ cycle inside the TS. In the heliosheath region, however, the difference can become significant, especially at lower energies. The modulation 'barrier' effect is clearly altered for 16 MeV galactic protons and negative radial gradients may occur at the current *Voyager 1* latitude and in the equatorial plane. For the $A < 0$ cycles even more significant differences occur, even inside the TS, although it becomes insignificant at Earth. The shock at 1 GeV is markedly more effective in the heliospheric nose region than in the tail region for the scenario where the V changes with latitude in the heliosheath for the $A < 0$ cycle and solar minimum conditions. The TS is clearly more effective in the nose region than in the tail region for the scenario where V changes with latitude in the heliosheath and even more in the equatorial regions than in the polar regions.

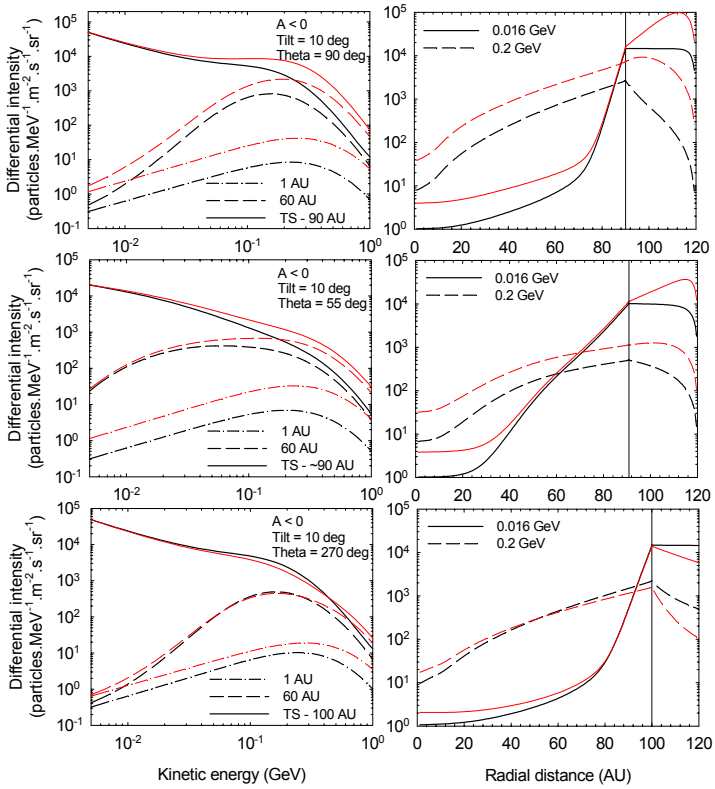

Figure 3. Similar to Fig 2 but for anomalous protons. For colour, see electronic version.

4. Acknowledgments

We thank the South African National Research Foundation and the Deutsche Forschungsgemeinschaft for partial financial support under the bilateral agreement, GUN #2049412 and DFG SCHL201/14-1/14-2/14-3. UWL wishes to thank the NRF for partial financial support during his post-doctoral studies.

References

[1] Borrmann, T., and Fichtner, H., Adv. Space. Res., submitted, (2005).
[2] Ferreira, S. E. S., Potgieter, M. S., and Scherer, K. Ap. J., 607, 1014, (2004).
[3] Fichtner, H., Space Sci. Rev., 95, 639, (2001).
[4] Florinski, V., Zank, G. P., Jokipii, et al., Ap. J., 610, 1169, (2004).
[5] Haasbroek, L. J., and Potgieter, M. S., Adv. Space Res., 19(6), 921, (1997).
[6] Langner, U. W., and Potgieter, M. S., J. Geophys.R., 109(A01103), 1, (2004a).
[7] Langner, U. W., and Potgieter, M. S., Annales Geophys., 22, 3063, (2004b).
[8] Langner, U. W., and Potgieter, M. S., Ap. J., in press, (2005).
[9] Langner, U. W., Potgieter, M. S., and Webber, W. R., J. Geophys.R., 108(A10), 8039, (2003).
[10] Langner, U. W., Potgieter, M. S., Fichtner, H., and Borrmann, T., Ap. J., submitted, (2005).
[11] Parker, E. N. 1965, Plan. Space Sci., 13, 9, (1965).
[12] Stone, E. C., and Cummings, A. C., Proc. 28th Inter. Cosmic Ray Conf., 3889, (2003).
[13] Zank, G. P., Space Sci. Rev., 89, 413, (1999).
[14] Zank, G. P., and Müller, H. R., J. Geophys. R., 108, SSH7:1, (2003).